Nucleic Acids Research, 2001, Vol. 29, No. 11 **2303–2313**

Parallel multiplex thermodynamic analysis of coaxial base stacking in DNA duplexes by oligodeoxyribonucleotide microchips

Vadim A. Vasiliskov[1,2], Dmitry V. Prokopenko[1] and Andrei D. Mirzabekov[1,2,3,*]

[1]Engelhardt Institute of Molecular Biology, Russian Academy of Sciences, 119991 Moscow, Russia, [2]Moscow Institute of Physics and Technology, 141700 Dolgoprudny, Russia and [3]Biochip Technology Center, Argonne National Laboratory, Argonne, 9700, south Cass Avenue, IL 60439-4833, USA

Received February 5, 2001; Revised and Accepted April 13, 2001

ABSTRACT

Parallel thermodynamic analysis of the coaxial stacking effect of two bases localized in one strand of DNA duplexes has been performed. Oligonucleotides were immobilized in an array of three-dimensional polyacrylamide gel pads of microchips (MAGIChips™). The stacking effect was studied for all combinations of two bases and assessed by measuring the increase in melting temperature and in the free energy of duplexes formed by 5mers stacked to microchip-immobilized 10mers. For any given interface, the effect was studied for perfectly paired bases, as well as terminal mismatches, single base overlaps, single and double gaps, and modified terminal bases. Thermodynamic parameters of contiguous stacking determined by using microchips closely correlated with data obtained in solution. The extension of immobilized oligonucleotides with 5,6-dihydroxyuridine, a urea derivative of deoxyribose, or by phosphate, decreased the stacking effect moderately, while extension with FITC or Texas Red virtually eliminated stacking. The extension of the immobilized oligonucleotides with either acridine or 5-nitroindole increased stacking to mispaired bases and in some GC-rich interfaces. The measurements of stacking parameters were performed in different melting buffers. Although melting temperatures of AT- and GC-rich oligonucleotides in 5 M tetramethylammonium chloride were equalized, the energy of stacking interaction was significantly diminished.

INTRODUCTION

Stacking interactions between adjacent bases located in the same strand play an important role in the formation of nucleic acid duplexes (1). Pieters *et al.* (2) and Snowden-Ifft and Wemmer (3) initiated detailed fundamental studies of the stacking interactions of two bases in DNA. In 1994, Turner and co-workers (4,5) started large-scale experiments to investigate coaxial stacking in the A-form of RNA and developed corresponding theoretical concepts. The Turner group conducted numerous melting experiments in solutions of RNA duplexes with different base interfaces (4,5). In addition, this group studied stacking in RNA containing mismatches of interface bases (6). The goal of these studies was to predict RNA folding.

A number of later works addressed the relationship between DNA stacking and its conformation (7–9). However, no comprehensive investigation comparable in scope to the work of Turner's group on RNA has been undertaken. Meanwhile, the A-form of RNA and the B-form of DNA have different relative arrangements of bases, and therefore stacking interactions in these structures should differ significantly.

An important feature of coaxial stacking is the absence of covalent linkage between the interacting bases. Hence, the energy of coaxial stacking interaction is substantially different from the parameters of interaction between the neighboring bases in the native B-form (9). It may depend not only on the nature of interacting bases, but also on their nearest neighbors, and may be even on longer stretches of flanking sequences.

A number of theoretical studies have been published attempting to quantitatively assess the thermodynamic parameters of stacking between two bases (1,10–17), including the impact of hydrophobic interactions. These models were able to provide only approximate values of the energy involved and to estimate relative strengths of interactions for different bases. In the future, these models might be able to take advantage of ever growing computing power to take into account all aspects of stacking interactions and offer more precise predictions (18).

Currently, an experimental approach remains the only reliable way to investigate stacking interactions. We are especially interested in one particular stacking phenomenon, which occurs at the interface between two bases in a DNA duplex interrupted by a single-strand nick, so-called coaxial stacking. The concept of coaxial stacking was first introduced by Lysov *et al.* in 1988 (19) as the rationale for Contiguous Stacking Hybridization (CSH). A number of research groups are developing the CSH approach, using biological microchips to detect mutations and to enhance the efficiency of Sequencing By Hybridization (SBH) (19–28).

*To whom correspondence should be addressed at: Engelhardt Institute of Molecular Biology, Russian Academy of Sciences, Vavilov strasse 32, 119991 Moscow, Russia. Tel: +7 095 1350559; Fax: +7 095 1351405; Email: amir@genome.eimb.relarn.ru

Previously, we were able to demonstrate that there is a direct correlation between the data obtained by melting DNA duplexes with one member immobilized on the three-dimensional microchip, on the one hand, and melting the same duplex free in solution, on the other (29; E.B.Khomyakova, unpublished results). Reasoning that individual gel pads of the microchip (MAGIChip™) (30) can be used as micro test tubes, we designed a special microchip to characterize coaxial stacking interactions. Further, we studied the coaxial stacking behavior of all 16 combinations of the four natural interfaces between bases. In addition, we carried out these experiments in several buffers known to affect melting properties of DNA duplexes with varying GC-content (31). We also characterized thermodynamic parameters of coaxial stacking of some modified bases, as well as mispaired bases and oligonucleotides carrying terminal modifications in the stacking zone (26).

The eventual goal of this study is to improve discrimination for on-chip mutation detection.

MATERIALS AND METHODS

Solvents and reagents were obtained from commercial suppliers and were used without further purification.

Oligonucleotides

All deoxyribonucleotides were synthesized on an ABI-394 DNA–RNA synthesizer (Applied Biosystems, Foster City, CA) using standard phosphoramidite chemistry. A 3′-amino group was introduced into 10mers by using 3′-Amino-Modifier C7 CPG (C7; Glen Research, Sterling, VA) during synthesis. A 5′-amino group was introduced into 17mers and 5mers by using 5′-Amino-Modifier C7 (Glen Research). Labeling of the 5′-amino group with fluorescein isotiocyanate (FITC) and Texas Red (TR) was performed following standard protocols (32). Pentamers were modified with phosphate at 3′-ends using chemical phosphorylation reagent (Glen Research). Decamers were modified at 5′-ends with phosphate, acridine, FITC, 5,6-dihydrouridine, or 5-nitroindole using standard amidites (Glen Research). Amidite for 5′-modification of 10mers with urea derivative of deoxyribose was synthesized as described elsewhere (33). Modified bases 2-amino-dA and N4-Et-dC, as well as terminal FITC substitutions in the 17mers, were introduced by using corresponding amidites (Glen Research). Unlabeled and fluorescently labeled oligonucleotides were purified by either reverse-phase liquid chromatography (HPLC), or by electrophoresis in denaturing polyacrylamide gels. HPLC (Gilson Inc., Middleton, WI) was done under the following conditions: C-18 Nucleosil column (Sigma, St Louis, MO), particle size 7 μm, 10–50% CH_3CN in 0.1 M triethylammonium acetate (TEAA; Fluka, Milwaukee, WI). After purification all oligonucleotides were controlled by MALDI-TOF mass spectrometry (27). Measurements were performed on KOMPACT-MALDI 4 (Kratos Analytical, Chestnut Ridge, NY).

Microchip design and manufacture

Microchips containing immobilized oligonucleotides within polyacrylamide gel pads were manufactured as described earlier (30,34,35). The standard microchips for fluorescence monitoring consisted of a rectangular arrangement of 0.1 × 0.1 × 0.02 mm gel pads spaced 0.2 mm apart. The scheme of oligonucleotide design can be found in Figure 1.

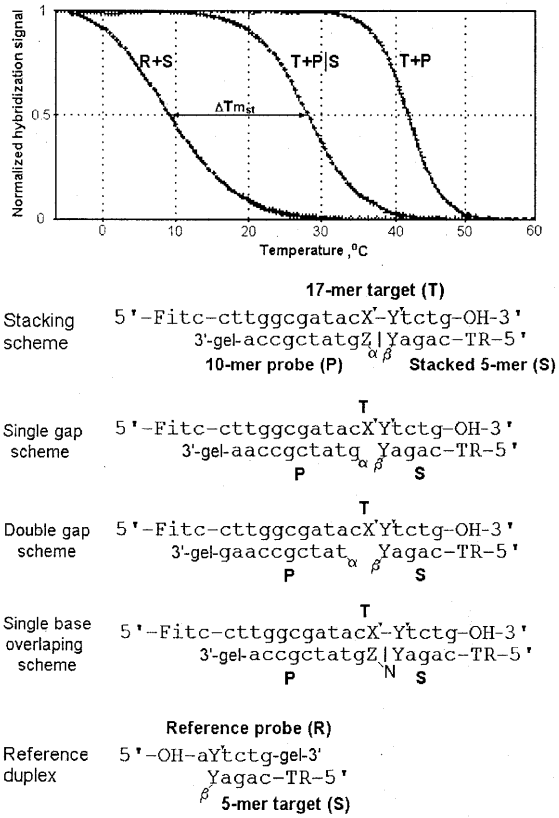

Figure 1. Typical melting curves and CSH hybridization schemes. For every pair X and Y, 1 μmol of 17mer target oligonucleotide T and 5 μmol of perfectly matched pentamer S were hybridized simultaneously in large excess to oligonucleotides P and reference pentamers R immobilized in gel pads of the microchip. Bases X, Y, Z, N = A, T, G, C, where base X′ is complementary to X, and Y′ is complementary to Y. Equilibrium melting curves of first transitions were registered using computer guided fluorescent microscope and excitation and emission filters for TR (curves R + S and T + P|S). Then melting curves of second transitions were registered on the same microchip in an independent experiment using microscope filters for FITC band (curve T + P). Melting curves represent coaxial stacking combination of perfectly matched interface bases (X, Y, Z = A; α, β = OH). Hybridization buffer i (see Materials and Methods).

The microchip had three subarrays of gel pads. The first subarray consisted of 6 × 9 pads containing immobilized 10mer probes (P) that formed duplexes with a target 17mer (T) for second transition (T + P). Each of the nine rows of gel pads (*a–i*) contained decamers P1–P6. Oligonucleotides P1–P4 have the following structure: 3′-gel-C7-accgctatgZ-α, where Z designates bases dA, dT, dC or dG, and α designates various groups as described below. Decamer P5 has the structure 3′-gel-C7-aaccgctatg-α and is designed to form a single nucleotide gap. Decamer P6 has the structure 3′-gel-C7-gaaccgctat-α and forms a double nucleotide gap. The rows differ in the α group: *a*, α = OH; *b*, α = PO_3; *c*, α = 5,6-dihydrouridine; *d*, α = urea derivative of deoxyribose; *e*, α = PO_3-C7-FITC; *f*, α = PO_3-C7-acridine; *g*, α = 5-nitroindole; *h*, α = C7-TR. An additional row *i* was designed to determine the stacking effect of modified bases, and it contained two decamers P1m and

P3m similar to P1–P6, where N is 2-amino-dA and N4-Et-dC, correspondingly.

The second subarray consisted of 4 × 4 gel pads with immobilized 11 base oligonucleotides PN1–PN16 with the following structure: gel-accgctatgZN-OH-5′, where Z and N are dA, dT, dG or dC. In this array Z indicates the position within each row and N indicates the row. Additional eleventh base N allows study of the stacking effect in duplexes with single base overlaps.

The third subarray consisted of 4 × 6 gel pads with immobilized reference oligonucleotides (R) to form reference duplexes (R + S) upon hybridization with 5mers in solution (P). This subarray had six (*a–f*) rows of four reference oligonucleotides R1–R4 each. These oligonucleotides differ by their dangling ends and immobilization position: *a*, 5′-OH-aNtctg-C7-gel; *b*, 5′-OH-Ntctg-C7-gel; *c*, 5′-gel-Ntctg-OH; and *d*, 5′-gel-cttggcgatactNtctg-OH, where N is dA, dT, dC or dG. Rows *e* (5′-OH-aNtctg-C7-gel) and *f* (5′-OH-Ntctg-C7-gel) consist of reference oligonucleotides R2m and R4m containing modified nucleotides (m) and are similar to rows *a* and *b*, where N is 2-amino-dA or N4-Et-dC, correspondingly. These oligonucleotides yield reference data for oligonucleotides P1m and P3m and modified target oligonucleotide T to study the stacking effect on modified bases.

Hybridization and melting

All experiments with microchips were performed in real time using an automatic experimental setup consisting of a two-wave-length fluorescent microscope (LOMO, Russia), CCD-camera (SenSys 1602E, 1024 × 1536 pixels; Roper Scientific Inc., Tucson, AZ), Peltier thermotable, temperature controller, and a computer equipped with a data acquisition board (29). The microscope had FITC and TR switchable excitation and emission filters (36). For experimental control and data processing, special software was designed based on LabVIEW virtual instrument interface (National Instruments, Austin, TX). All hybridizations were carried out in a hybridization chamber with a working volume of 200 µl. The total exposure time did not exceed 2 min (no more than 130 acquisitions during the time course of an experiment were made at 1–1.5 s per measurement). It was much shorter than the characteristic half-time of photobleaching (~1 h) determined for the fluorescent labels used.

Hybridization experiments were performed in different buffers: (i) 1 M NaCl, 10 mM $NaHPO_4$, pH 7.0; (ii) 1 M NaCl in 10% MeOH, 10 mM $NaHPO_4$, pH 7.0; (iii) 1 M TEAA, pH 7.0; (iv) 5 M betaine monohydrate (Sigma Chemical, St Louis, MO), 1 M NaCl, 10 mM $NaHPO_4$, pH 7.0; (v) 5 M TMA chloride (Merck, Darmstadt, Germany), 4 M urea, 10 mM Tris–HCl pH 7.0; (vi) 0.1 M NaCl, 10 mM $NaHPO_4$, pH 7.0. For some experiments, additional components were added: 5 mM EDTA, 0.1% Tween-20 or 0.01% Triton X-100.

The hybridization chamber was cooled to 0°C (buffer 6), –5°C (buffers 1 and 3) or –10°C (buffers 2, 4 and 5) for a period of time sufficient to reach maximum signal. In control experiments the curves of annealing and melting of the duplexes were virtually identical. Therefore, we considered these curves to be equivalent and refer to them as equilibrium melting curves.

Equilibrium melting curves were registered at increasing temperature at a continuously increasing rate from 1°C per 40 min at low temperatures (–10°C) to 1°C per 2 min at high temperatures (+50 to +70°C). The time to reach equilibrium was determined as the time required for the hybridization signal to reach a plateau after a stepwise temperature change.

The total amount of labeled oligonucleotides in hybridization solution (1 nmol) was maintained in large excess with respect to the amount of immobilized oligonucleotides, which was in the range of 0.03–0.06 pmol per gel pad, as described earlier (29). Both large excess and large volume of solution were used to diminish the changes in concentration caused by the penetration of pentamer S and 17mer T into the gel pads and by adsorption to the walls of the hybridization chamber. Vast excess of the oligonucleotides in solution significantly increased the accuracy of experiments, and the concentration of free target oligonucleotides could be considered constant at all temperatures for the sake of further data processing.

Comparative melting experiments in solution were performed on a Jasco-V-550 UV/VIS spectrophotometer (Jasco Corp., Tokyo, Japan) equipped with a Peltier thermo-cuvette guided by a thermo-controller and computer. Optical path length was 0.1 cm. Melting curves were recorded at wavelength 260 nm. The temperature was increased at the rate of 0.5°C per min from –5 to 95°C in hybridization buffer 1 at oligonucleotide concentration 10 µM.

Image processing and melting curve analysis

Data processing and melting curve analysis were performed as described earlier (29).

The hybridization buffer contained 1 µM of 17mer T and 5 µM of perfectly matched pentamer S. The 17mer target oligonucleotide T can form duplexes with immobilized oligonucleotides P on the microchip, and consequently its dangling end can form contiguously stacked duplex with the pentamer S (Fig. 1). Alternatively, oligonucleotide T can form duplexes with the pentamer S in solution, resulting in a significant change in the acting concentration of pentamer during hybridization and melting. To avoid this, each pentamer was added at 5-fold excess with respect to the concentration of the 17mer T. In these conditions, possible change of free pentamer concentration in solution during melting experiments can cause only limited distortion in melting curves, not exceeding a shift of 1°C in melting temperatures (T_m).

The resulting melting curves were analyzed by two-stage mean square regression, assuming that they fit ideal S-shaped transition curves. First, the tunnel cut-off method was used to automatically discard erroneous experimental points (<1–5%). These erroneous data were caused by dust or bubbles in the hybridization solution. Then a second regression analysis was applied to improve the accuracy of the data.

T_m and ΔG_{37} values for a given microchip were determined as defined earlier (29). Stacking contributions were calculated for each (X|Y) combination independently, subtracting ΔG_{37} and T_m values of reference duplexes from ΔG_{37} and T_m obtained for stacking duplexes in the same experiment.

RESULTS

Thermodynamic analysis of coaxially stacked duplexes on the microchip

To measure stacking interactions for different interfaces in contiguous oligonucleotide duplexes, we compared their thermodynamic parameters to reference duplexes formed without stacking partners. The scheme of our experiments together with examples of melting curves are shown in Figure 1. A 2-fold difference in the length of duplexes made the transitions (T + P) and (R + S or T + P/S) of the complex thermodynamically independent. Figure 2 presents our main results after conversion of melting curves into thermodynamic parameters as described in the Materials and Methods. For each base interface X | Y, results were obtained in a separate experiment and are shown in one of 16 cell diagrams. Values of the coaxial stacking effect between perfectly paired bases are plotted as the first, second and third bar of each of 16 diagrams where Z = X.

The stacking effect was determined as follows:

$$\Delta T_{\text{m stacking}} = T_{\text{m stacking}} - T_{\text{m reference duplex}}$$

$$\Delta\Delta G_{\text{stacking}} = \Delta G_{\text{stacking}} - \Delta G_{\text{reference duplex}}$$

In each case the T_m or ΔG of reference duplex with pentamer S (curve R + S) was subtracted from the T_m or ΔG of stacked, gapped or overlapped 5mer obtained in the same experiment. This approach enabled us to ignore the effect of hydrogen bonding in calculating the thermodynamic parameters of stacking.

Figure 2A shows $\Delta\Delta G_{37}$ values. Figure 2B shows ΔT_m values. The presence of terminal phosphates on the 5′-end, or even 3′- or 5′-ends simultaneously, had negligible effect on stacking. Data represented by the first bars in each cell for α = OH and β = OH were obtained in a separate series of experiments, using pentamers without 3′-terminal phosphates and immobilized oligonucleotides with α = OH. This microchip had been designed for preliminary test experiments. All other data were obtained on another microchip, containing oligonucleotides with all α, as described in the Materials and Methods. Results obtained with these two different microchip designs were very similar, thus confirming the reproducibility and dependability of MAGIChips™.

The results shown in Figure 2 are further summarized in Table 1. The main conclusion of these experiments is that coaxial stacking of 3′-adenine (Y position, where adenine is at the 3′-end of pentamer S) with any 5′-base of the 10mer P is stronger than between any other bases. Adenine located at the 5′-side of immobilized 10mer P (X position, X′ = T) shows a similar tendency, although to a somewhat lesser extent.

Additional control experiments showed that stacking did not depend on pH (from 6.0 to 8.0), addition of EDTA (up to 1 mM) or surfactants Triton X-100 (up to 0.1%) and Tween-20 (up to 1%). Changing salt concentration from 1 to 0.1 M did not affect the stacking significantly; similarly, using a 17mer T to pentamer S ratio of 1:2 instead of 1:5 had no effect. In addition, we made a special chip using polyhydroxyethylacrylate instead of polyacrylamide gel in pads (monomer was at the same concentration of 5%). The stacking effect on such a chip was the same. Therefore, amide groups of the polyacrylamide gel do not interfere with stacking.

Table 1. Comparison of ΔT_m values (coaxial stacking effect) for all combinations of standard bases

3′	5′			
	A	T	C	G
A	20 (+9, +4)	11 (+4, +2)	6 (+2, 0)	9 (+6, +5)
T	16 (+5, +1)	12 (+3, +1)	3 (–2, –2)	8 (+4, +2)
C	17 (+8, +4)	13 (+2, –1)	4 (–1, –3)	6 (+2, –1)
G	16 (0, –1)	6 (–4, –7)	2 (–5, –7)	4 (0, –2)

The table summarizes relative coaxial stacking effects shown in Figure 2A and assessed by ΔT_m°C. The rows represent the base on the 3′-side (X), the columns the base on the 5′-side (Y). The first number in each cell corresponds to the X | Y interface for the given intersection. The numbers in parentheses correspond to maximum and minimum values of coaxial stacking effects among three remaining mismatched bases. Experimental error is 1°C.

Thermodynamic analysis of coaxial stacking in duplexes with mismatched interface bases

The ability of coaxial stacking to discriminate mismatches is very useful for mutation detection. Figure 2 shows thermodynamic data for four coaxially stacked pentamers (Y) forming all possible 5′-terminal mismatched interfaces. The results are displayed as the first three bars in each sub-cell for Z = A, T, C, G; Z ≠ X, in the stacking scheme of duplex 5′….X′-Y′….3′/3′….Z|Y….5′. For reference, it has to be compared to the stacking of the corresponding complementary paired base (Z = X). These melting data are summarized in Table 1. The data suggest that for all interface combinations the discrimination is high enough to detect any mutation of the interface bases. In some cases mismatch discrimination between pentamers stacked to perfect and to terminally mismatched bases is even higher than that between stacked pentamers and their reference duplexes. Even more efficient discrimination can be achieved, if mutation occurs on the side of 5mer. In this case, discrimination results from both diminished stacking with mispaired base and from diminished duplex energy due to missing hydrogen bonds. Among all mispaired bases, guanine (Z = G) at the 5′-ends of immobilized decamers had the maximum stacking effect in combination with all terminal bases Y of pentamers (gel-oligo9-Z|Y-oligo4-TR).

Thermodynamic behavior of reference duplexes on the microchip

The microchip had several types of oligonucleotides forming reference duplexes (R). These duplexes provide ‘base lines’ in each experiment, since their thermodynamic properties are used to calculate $\Delta\Delta G$ and ΔT_m values for stacked duplexes. Gel pads with immobilized reference oligonucleotides 5′-OH-aNtctg-C7-gel (N = A, T, C, G in oligonucleotide *a*) can form reference duplexes with 5mers with adenine dangling at their 5′-end. This dangling end should compensate for the impact of dangling bases, primarily the first one, which remains on 17mer target T in the duplex T + P after the completion of the first transition (first melting of the complex T + P|S). A

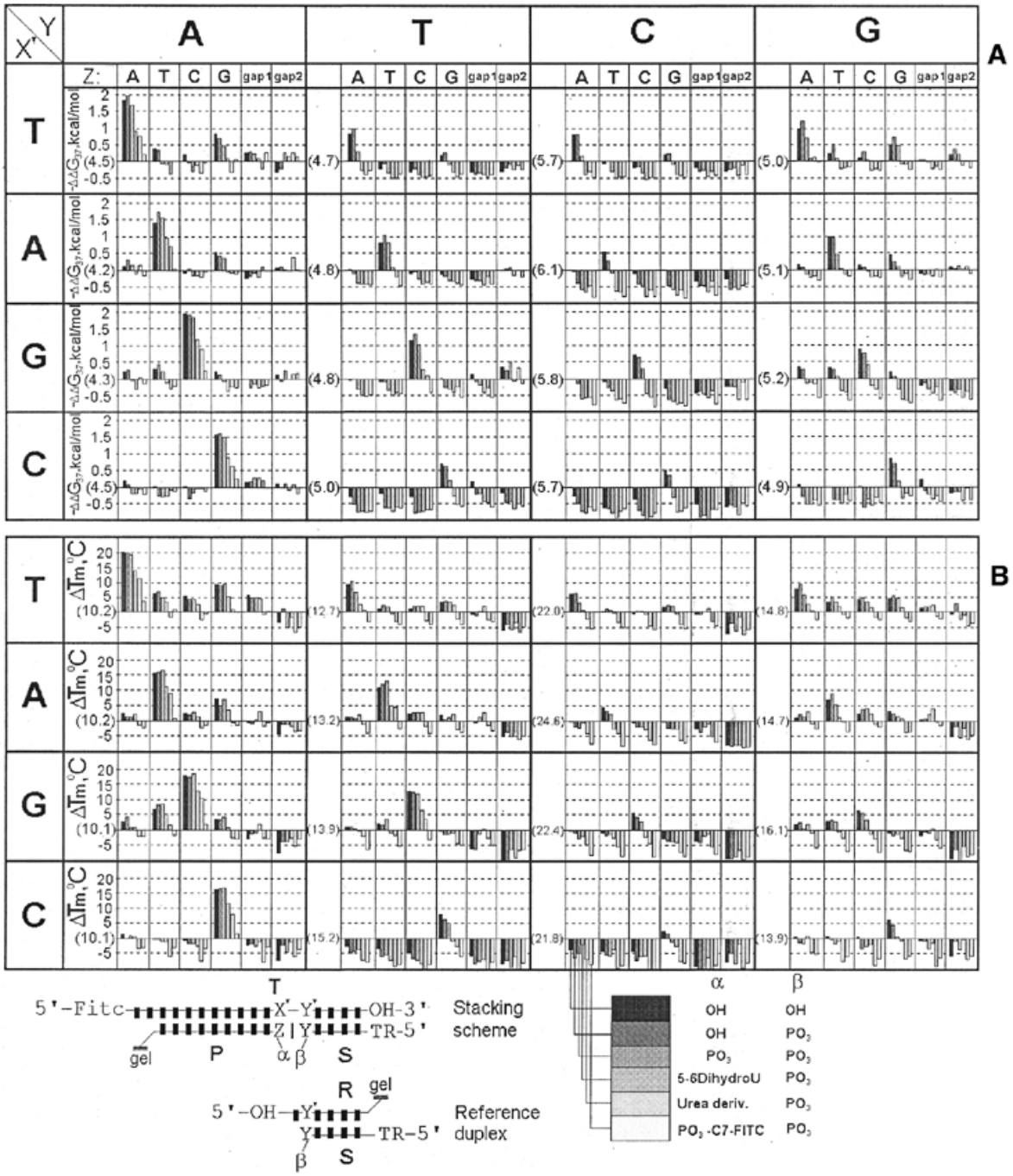

Figure 2. Parameters of the stacking effect in the presence of different 5′- and 3′-modifications. (**A**) Free energies $\Delta\Delta G_{37}$; (**B**) melting temperatures T_m. For a given pair X, Y, 1 µmol of 17mer target T (5′-FITC-C7-cttggcgatacX′Y′tctg-OH-3′) and 5 µmol of perfectly matched pentamer S (3′-βYagac-C7-TR-5′) were hybridized simultaneously in large excess with the microchip. Data are shown for five rows of six immobilized oligonucleotides P only, ranged by α. P1–P4 have the following structure: gel-accgctatgZα-5′; P5, gel-aaccgctatgα-5′; P6, gel-gaaccgctatα-5′; and four reference pentamers R1–R4, 5′-OH-aY′tctg-gel. Bases X, Y, Z = [A, T, G, C], where base X′ is complementary to X and Y′ to Y. The residue α = (i) OH, (ii) PO_3, (iii) 5,6-dihydroU, (iv) urea derivative from deoxyribose, or (v) PO_3-C7-FITC. Equilibrium melting curves of the first transition were registered by a computer guided fluorescent microscope with TR settings. The melting experiment was repeated 16 times using all possible combinations of bases 5′….X′Y′/Z|Y….5′ adjacent to the stacking zone. These series were done for α = OH (data shown only for α = OH) and for β = PO_3 (for all α). Hybridization buffer i (see Materials and Methods). All melting curves were approximated by ideal S-shaped transition curves using regression analysis, and relative $\Delta\Delta G_{37}$ and ΔT_m values obtained from each experiment were calculated as shown below and plotted as bar graphs: (i) $\Delta\Delta G_{37}$ (X, Y, Z, α, β) = $\Delta G_{37\,\text{stacking}}$ (X, Y, Z, α, β) − $\Delta G_{37\text{reference duplex}}$ (Y, β), and (ii) ΔT_m (X, Y, Z, α, β) = $T_{m\,\text{stacking}}$ (X, Y, Z, α, β) − $T_{m\,\text{reference duplex}}$ (Y, β). Absolute values of ΔG_{37} and T_m of the reference duplex (Y, β = PO_3) are indicated near each zero line in parentheses. Mean square errors were 0.2 kcal/mol and 1°C, correspondingly.

dangling adenine gives maximum stabilization among all dangling ends (18) and therefore can serve as the highest possible estimate of energy change. For N = Y′, duplexes with dangling adenine had the highest T_m and ΔG values among all

reference duplexes formed by oligonucleotides *a–d* (see Materials and Methods). The stabilizing effect of the dangling adenine results in a T_m increase of reference pentamer duplexes by 4–5 degrees in comparison with duplexes formed by pentamers *b* and *c*.

The difference between thermodynamic parameters of duplexes formed by *a* on one hand, and *b* and *c* on the other, is in agreement with Bommarito *et al.* (18) (data not shown). Therefore, duplexes formed by oligonucleotide *a* were used as references in obtaining the stacking data in Figure 2. Absolute T_m and ΔG_{37} values of reference duplexes in each of 16 experiments for $\beta = PO_3$ are presented near the zero line of each bar graph [X, Y]. For β = OH, ΔG_{37} and T_m values were similar (data not shown). Adding PO_3 group at the 3′-ends of hybridized pentamer caused no appreciable effect on thermodynamic parameters.

It has to be noted that in each column of Figure 2 the same pentamer was used for four separate experiments with different 17mers. The reproducibility of the experiments can be assessed by comparing base line values of reference duplexes for different experiments. Our actual estimates of errors in determining $\Delta\Delta G$ and ΔT_m in stacking experiments are even lower, since they do not include those errors in the studies of reference duplexes that are caused by thermostable shift and changes in oligonucleotide concentrations.

Oligonucleotides *b* (5′-OH-Ntctg-C7-gel) and *c* (5′-gel-C7-Ntctg-OH) were designed to test whether the attachment site affects the melting behavior of the duplexes. We determined that T_m and ΔG values were similar to within ±1°C and ±0.1 kcal/mol, respectively. Therefore, duplex energy does not depend on which end is used for immobilization.

Termination of stacking by extension with different compounds

Figure 2 shows that two terminal phosphates between interface bases diminished (terminated) the stacking effect relatively poorly. The effects of 5,6-dihydrouridine and urea derivative of deoxyribose were somewhat stronger. For all X, Y, Z the strongest suppressor of stacking interaction was FITC attached to the end base of the immobilized oligonucleotide. Generally, all three compounds, 5,6-dihydrouridine, urea derivative and FITC, did not stabilize gaps, in contrast to all standard bases.

Thermodynamic parameters of second transitions were measured in additional control experiments. It was found that FITC, as well as other terminal groups used in the study, did not shift the transitions, which occurred at 43–45°C in 1 M NaCl (see Fig. 1). Therefore, the suppression of stacking termination by FITC does not involve destabilization of double helix (T + P). Other explanations might be either strong hydrophobic interactions with the dangling end of the single strand that compete with stacking; or strong non-specific stacking of FITC to the adjacent base Z due to the absence of polar groups in FITC residues that could prevent the formation of the strong hydrophobic bond Z|Y.

On the contrary, acridine residue attached in place of FITC through the same amino group increased the temperature of transition (T + P) by 3–6°C. This effect was suppressed in 1 M NaCl. In addition, acridine can stabilize single base gaps, probably by inserting itself as a regular base (data not shown). Another known intercalator, phenazinium (37), did not stabilize either stacking or gaps to the extent found in the case of acridine. Depending on the nature of stacking interface, acridine acted as either a weak suppressor or, more rarely (in some G|C interfaces), as a weak enhancer. This study was done in parallel on the same large-scale chip for all 16 combinations of base interfaces X|Y, in 1 and 0.1 M NaCl (data not shown). In all cases, stacking mismatch discrimination (difference between stacking effects in perfectly paired sequences as compared to all three mispaired bases) was poor in 1 M NaCl and slightly better in 0.1 M NaCl.

The same screening was done for the universal base 5-nitroindole, which was attached to immobilized 10mer oligonucleotide P by a regular phosphodiester bond. In contrast to acridine, 5-nitroindole did not stabilize gaps, and it did stabilize regular duplex (transition T + P). In case of gaps, 5-nitroindole can probably turn away and intercalate into the duplex T + P. In addition, 5-nitroindole significantly improved stacking with mispaired interface bases at terminal positions of P, reducing stacking mismatch discrimination. In this case it probably intercalates into the nick.

We attempted to characterize the effect of TR on stacking by the same approach that had been used for FITC. Unfortunately, we could not obtain valid melting curves for TR-labeled 5mers S (data not shown), because immobilized 10mers P were also labeled with TR and emitted too high background signal to achieve sufficient accuracy. We could not obtain good melting curves using FITC-labeled 5mers S either, because FITC emission is not stable enough and depends too much on temperature. Additionally, there is a transfer of energy between FITC and TR. Therefore, we conducted other tests, attaching TR at the 3′-ends of pentamers, which served as a potential stacking suppressor and fluorescent label simultaneously (data not shown). In these experiments, TR diminished stacking approximately to the same extent as FITC, or slightly less. In addition, in gel pads containing immobilized decamers with FITC at their 5′-ends, a strong non-specific stabilization of stacking by 3′-TR ends of pentamers took place. Probably, there was a strong interaction between TR and FITC outside the oligonucleotide duplex.

Comparison of stacking effects in gel and in solution

Four typical control points of coaxial stacking with perfectly matched interface bases were processed in a spectrophotometer cuvette, and they were compared with those obtained on microchips (Fig. 3). Oligonucleotides with the same sequences were used on the microchip and in solution. Second transitions in solution, in contrast to the microchips, occurred in hairpins introduced for this purpose in the target oligonucleotide. By using hairpins we avoided the potential inequality in the concentrations of complementary strands, which in turn could distort melting data. As a result, we were able to achieve a good correlation between microchip and solution data.

Thermodynamic analysis of gaps and single base overlaps of perfectly matched and mismatched bases

Thermodynamic data for single and double gaps are shown in Figure 2 (Z = gap1 or gap2). The thermodynamic parameters of single gaps are similar to reference duplexes (zero line). Therefore, a single gap does not cause significant distortion of a regular 5mer duplex. Furthermore, one can conclude that stacking is a short-range interaction. However, double and longer gaps, as well as long stems, incur some destabilization

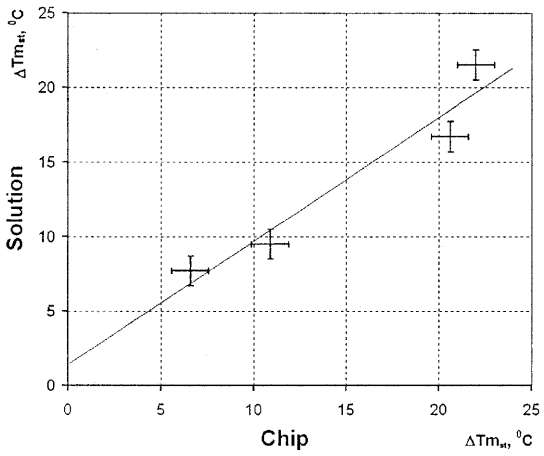

Figure 3. Correlation between measurements of the stacking effect (ΔT_m) on microchips and in solution. Abscissa corresponds to the results obtained on microchips, ordinate in solution. For the experiments on microchips, 1 µmol of target 17mer T 5′-FITC-C7-cttggcgatacX′Y′tctg-OH-3′ and 5 µmol of perfectly matched pentamer S 3′-OH-Yagac-C7-TR-5′ were hybridized simultaneously in large excess with microchip. For the graph shown here, only data from pads containing oligonucleotides gel-accgctatgZ-OH-5′ were used. Stacking interface bases were perfectly paired (Z = X) for base combinations [X, Y] = [T, A], [C, A], [C, G], [G, C]. Base X′ is complementary to X, and Y′ to Y. Equilibrium melting curves of the first transition were registered by a computer guided fluorescent microscope with TR settings. For the experiments in solution, 10 µmol of hairpin oligonucleotide 5′-OH-Xgtatcgccaag-tttt-cttggcgatacX′Y′tctg-OH-3′ and 10 µmol of perfectly matched pentamer 3′-OH-Yagac-C7-TR-5′ were mixed and hybridized in a cuvette for [X, Y] = [T, A], [C, A], [C, G], [G, C]. Ten micromoles of two pentamers, which were used on the microchip, 3′-OH-Yagac-C7-TR-5′ and 5′-OH-Y′tctg-C7-NH-3′, were hybridized in a cuvette to serve as reference duplexes. Equilibrium melting curves of transitions were registered by UV spectrophotometer. All melting curves were obtained in hybridization buffer 1 and approximated by ideal S-shaped transition curves, using regression analysis, and relative ΔT_m values obtained from each experiment were calculated and plotted as shown below: $\Delta T_{m\ stacking}[X, Y] = T_{m\ stacking}[X, Y] - T_{m\ reference\ duplex}[Y]$. Mean square error was 1°C.

effect. It can be explained by interaction of ballast single-stranded sequences with those parts of oligonucleotides that play an important role in the formation of perfect duplexes (38).

The effect of long single base sequences on duplex stability was also tested in another way. A set of special reference oligonucleotides *d* (5′-gel-cttggcgatactNtctg-OH) similar to target oligonucleotide T was designed to test the effect of a long single-stranded sequence inserted between the duplex and immobilization point. Such ballast oligonucleotide sequence helped us to assess the stability of 5mer duplex formed at the end of a long ssDNA at a significant distance from another duplex comprising the immobilized oligonucleotide (27). Just two unpaired bases present in double gaps stacking schemes were sufficient to cause some destabilization of the adjacent duplex (see Fig. 2). A comparable destabilizing effect caused by two base and longer single-stranded inserts was observed when oligonucleotides *a, b* and *c* were tested (data not shown).

Some applications used for sequence proofreading and mutation detection by hybridization are based on the tiling method (27,28). Therefore, it is important to study single base overlaps, which can occur in these experiments. We tested the thermodynamic impact of these overlaps using microchip technology. Figure 4 presents free energy values for all combinations of overlaps and includes a comparison with regular stacking. These data are further summarized in Table 2.

Overlapping results in competition between two processes: turning out of the base N and turning out of the base Y (see legend to Fig. 4). Evidently, in all cases the competition between two perfectly paired bases or, more precisely, superposition of two coaxial stacking contacts (X|Y with turned out N and N|A with turned out Y) is energetically not favorable. This enables one to easily discriminate a frameshift stacking. The effect of perfectly paired bases is comparable to stacking suppressors, like FITC. Unfortunately, some terminal mispaired bases N do not suppress stacking interaction significantly (for example, see X′ = G, Y = G, Z = X = C, in the duplex 5′-oligo9-G-C-oligo4-3′/3′-oligo9-CN|G-oligo4-5′ for N ≠ G) (Fig. 4). An interesting situation occurred with some immobilized oligonucleotides that contained two terminal mismatched bases (Z and N) at the end position of P in the duplex P-T. For example, in the case of X′ = T, Y′ = T, Z = T, C, or G, Y = A, terminal N = A, which should be overlapped with Y = A (underlined in duplex 5′-oligo9-T-T-oligo4-3′/3′-oligo9-Z<u>A</u>|A-oligo4-5′) probably shifted one base to the left instead of leaving Z base unpaired. It became perfectly paired to X′ = T, while Z = T probably protruded. So, Y = A of pentamer S developed an energetically favorable stacking interaction with such 'shifted' N = A (see second bars for X′ = T, Y = A, Z = T, C or G).

Influence of equalizing agents on the stacking effect and mismatch discrimination

A number of agents have been tested that equalize the stability of G/C and A/T duplexes, such as TMA, TEAA (31) and betaine (39). Unfortunately, in all cases the equalizing effect was accompanied by a significant decrease in the energy of stacking interactions (data not shown). Therefore, the use of the tested equalizing agents in contiguous stacking experiments compromises the efficiency of this approach.

Influence of base modification on the stacking effect and mismatch discrimination

Another approach to AT/GC-equalization is the introduction of modified bases in the duplex. Currently, two commercially available base analogs are often used for duplex equalization: 2-Amino-dA (A*) and N4-Et-dC (C*). To achieve the desired effect, every modified base should substitute for its natural analog in the duplex structure under investigation. Since coaxial stacking may take place in such substituted complexes, it seems important to compare stacking interactions of natural and modified bases. In this study, we successively replaced all As and Cs with A*s and C*s in the ultimate and penultimate positions of the stacking interface X|Y. Natural and modified oligonucleotides were tested both on the microchip and in solution in four independent melting experiments. For all 16 possible bases, 64 independent melting experiments were conducted (data not shown). In all cases thermodynamic parameters of stacking with modified bases were very similar to previous data obtained for natural bases and shown in Figure 2. In most cases, we observed minor gradual decrease in average stacking if we successively replaced all As and Cs in the interface with modified A*s and C*s. In the course of these experiments we found it possible to equalize the T_m values of

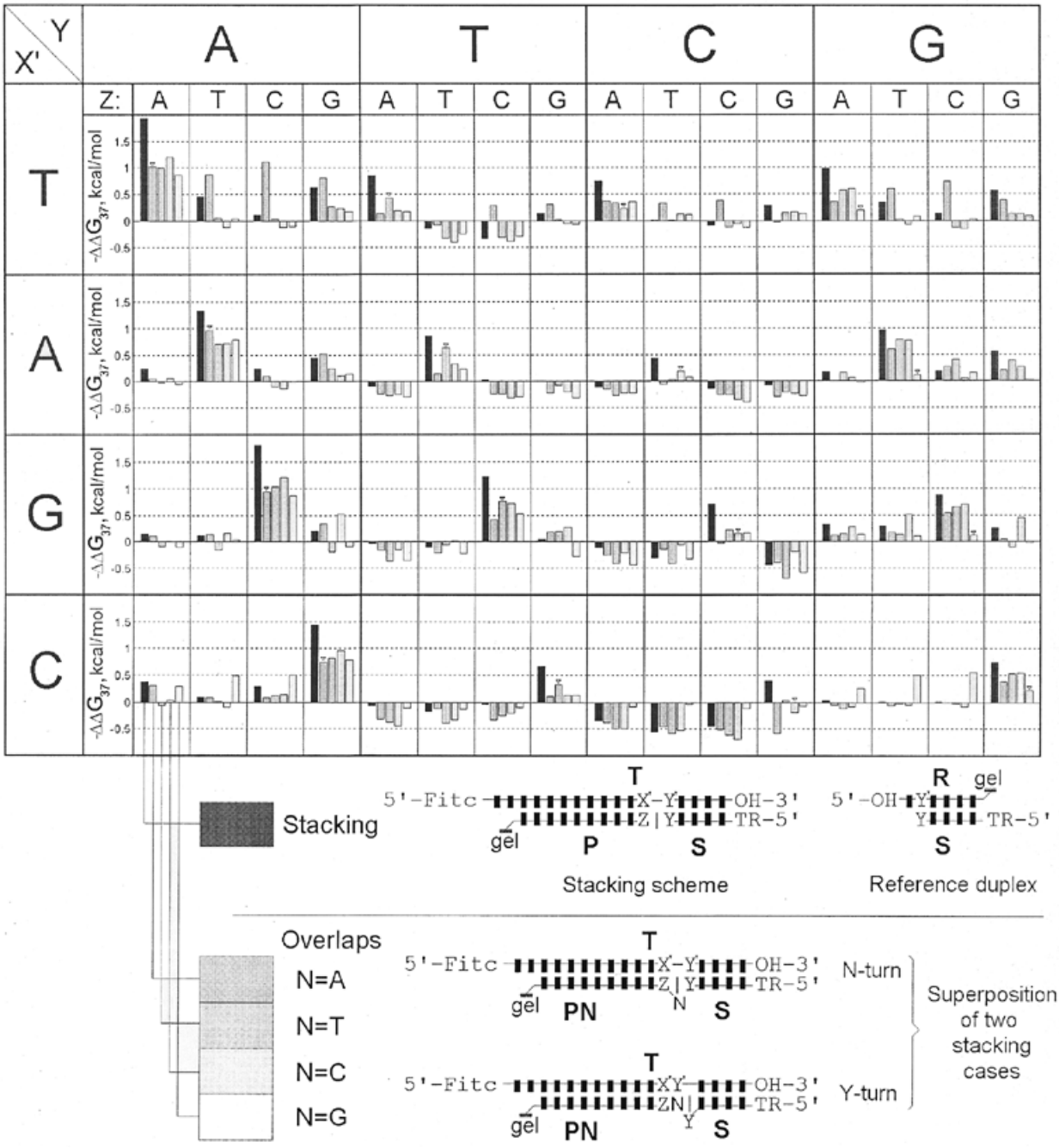

Figure 4. Stacking effect at interfaces with single base overlaps. For a given pair X, Y, 1 µmol of 17mer target T 5′-FITC-C7-cttggcgatacX′Y′tctg-OH-3′ and 5 µmol of perfectly matched pentamer S 3′-OH-Yagac-C7-TR-5′ were hybridized simultaneously in large excess with microchip. For a given Z, the first dark bar among all five bars in each sub-cell represents the data for coaxial stacking to perfect and mismatched bases of the four immobilized oligonucleotides P1–P4 gel-accgctatgZ-OH-5′ without overlaps. For all combinations of X and Y, the strongest stacking effect is observed between two perfectly paired bases. The remaining four light bars correspond to stacking of pentamers S to 16 different oligonucleotides PN1–PN16 (gel-accgctatgZN-OH-5′) containing one additional terminal base N overlapping with base Y of pentamer S to test whether it can reduce stacking. For given X and Y, the competition between two perfectly paired overlapping bases Y = N is shown by a small triangle over the bar. To assess the relative stacking effect, four reference pentamers R1–R4 (5′-OH-aY′tctg-gel) were immobilized on the same microchip. Bases X, Y, Z are A, T, G, or C; X′ is complementary to X, and Y′ to Y. Equilibrium melting curves of the first transition were registered using TR settings as described in the Materials and Methods. Melting experiments were repeated 16 times in hybridization buffer 1 with all possible combinations of bases 5′….X′Y′/ZN|Y….5′ adjacent to the stacking zone. Melting curves were approximated by ideal S-shaped transition curves using regression analysis, and relative $\Delta\Delta G_{37}$ values obtained for each experiment were calculated as shown below and plotted as bar graphs: $\Delta\Delta G_{37}(X, Y, Z, N) = \Delta G_{37\ stacking}(X, Y, Z, N) - \Delta G_{37reference\ duplex}(Y)$. Mean square error was 0.2 kcal/mol.

all four pentamer duplexes with variable terminal base content. The resulting equalization has been achieved without any appreciable loss in stacking strength. Unfortunately, equalizing behavior of modified bases is not always predictable,

Table 2. Comparison of ΔT_m values of coaxial stacking effect between perfectly paired interface bases and stacking effect with single base overlaps

3′	5′			
	A	T	C	G
A	20 (12)	10 (3)	6 (4)	9 (–1)
T	16 (4)	12 (8)	5 (–2)	7 (5)
C	17 (3)	14 (6)	6 (1)	8 (5)
G	16 (5)	7 (3)	3 (1)	6 (–4)

The table summarizes data obtained in experiments with single base overlaps (Fig. 4). Relative values of stacking effect without overlaps were obtained from another experimental series and are similar to the data shown in Table 1. For any given pair X and Y, ΔT_m of coaxial stacking effects in the presence of terminal overlapping base N = Y in the immobilized 11mer PN is shown in parentheses near reference value. Experimental error is 1°C.

especially in terminal positions. There is no model yet to calculate thermodynamic parameters of modified bases with the same precision that is already possible for natural bases (40). Therefore, the use of modified bases requires additional preliminary experiments for the proper choice of base modifications. Finally, in all cases the power of terminal mismatch discrimination in modified duplexes was approximately the same as in natural duplexes.

DISCUSSION

Direct measurement of stacking interaction energy in intact DNA or RNA duplexes is rather difficult and requires the development of elaborate physical models. The assessment of thermodynamic parameters of stacking interactions in coaxial duplexes separated in two parts by removing phospodiester bonds between nucleotides in one strand seems, on the contrary, quite straightforward. The lengths of the separated fragments of the interrupted strand must differ sufficiently in order to monitor and analyze the separated transitions. Therefore, the melting process of such complexes is non-cooperative, consisting of two independent stages (Fig. 1). The melting of the short duplex in such complexes is affected by its interaction with the longer strand at their interface, where the short duplex can be stabilized by stacking interaction and dissociate at a higher temperature. This approach enabled us to analyze the effect of base substitutions, modifications, deletions and insertions on stacking interaction by comparing it with the melting process of non-stacked (reference) duplex. Figure 1 illustrates different schemes of coaxial stacking and typical melting curves.

Thermodynamic parameters of reference duplexes closely correlate with published values calculated using the NN1 model (40) (data not shown).

It has to be noted that after a coaxially stacked pentamer S has melted away during the first transition, the 17mer T is left with a 5 nt dangling end. As a result, the first dangling base of T is probably loosening its 'B-form-like' conformation, and this process is accompanied by energy change, with some contribution by the four remaining dangling nucleotides as well. At the same time, the former interface base of the immobilized 10mer P becomes the last, resulting in additional redistribution of stacking energy. These considerations emphasize fundamental differences in the thermodynamics of stacking interactions in canonical B-form DNA, in coaxial stacking and in stacking of dangling ends.

In this work, we employed MAGIChips™ to obtain comprehensive characteristics of contiguous stacking interactions. Acrylamide gel pads of the MAGIChips™ can serve as microcuvettes for precise measurement of the thermodynamic parameters. This opens a broad field of microchip applications, studying the stacking interactions of various bases and DNA binding ligands. In particular, the possibility of obtaining thousands of melting curves simultaneously in real time enables one to investigate the impact of several bases flanking the immediate contacting partners. Using MAGIChips™ this seems quite feasible, similar to our present investigation of stacking interactions.

Coaxial stacking of adenine with other bases is stronger than stacking of other bases. The same phenomenon has been observed by Bommarito *et al.* (18) who studied the contribution of single base dangling ends to the stability of duplexes. In case of dangling ends, similar to coaxial stacking, the orientation of interface bases can deviate from canonical B-form (9). While dangling bases are unpaired and have no immediate neighbors in rigid conformation, interface bases in coaxial stacking are bound with the complementary strand and do have flanking bases. This explains why coaxial stacking effects (shift in T_m and ΔG) are approximately two times higher than the stacking energy estimates for dangling ends. Coaxial stacking involves not only interaction with the base on the other side of the nick, but with two other bases as well: one that is paired to the interface base in the opposite strand, and the other that is flanking it in the same strand.

According to Bommarito *et al.* (18), the high impact of adenine in the energy of coaxial stacking is defined mostly by the interaction of the bases that form the interface, with a lesser impact of flanking bases and bases paired to the interface bases in the complementary strand. The energy impact of adenine is asymmetric in terms of interface geometry. This notion can be illustrated by comparing data for [X, Y] = A, A on the one hand, and T, T on the other. The nick between A|A in duplex 5′….A|A….3′/3′….T-T….5″ is not equivalent to the nick between T|T in duplex 5′….T|T….3′/3′….A-A….5′ for AA/TT pair, as it was presented for two duplex base pairs XY/X′Y′ in the NN1 (nearest neighbor) model (41) for calculation of thermodynamic parameters of usual non-nicked duplexes in B-form (see table 3 in 40). It can probably be explained by a deviation of the interface bases separated by a nick from canonical B-form. Alternatively, adjacent bases may influence the stacking energy due to increased flexibility of nucleotides at the nick.

Studies have been published on model nicked structures containing coaxially stacked bases in solution (2,3,9). Conformation of the duplex around the nicked region was determined using NMR, and only slight local distortion and increased flexibility was found around the nicked region of the duplex. Maybe these conformational changes are sufficient to affect the thermodynamic behavior of the canonical B-form, and therefore we cannot obtain B-form-like symmetry for coaxially stacked bases. Specifically, the nick 5′-X′Y′/X|Y is not energetically equivalent to the nick 5′-X′|Y′/XY. Evidently, a

broken phosphodiester bond gives bases additional conformational mobility in comparison with B-form, and their actual position is defined by new minimum energy. Another reason for this asymmetry is probably a stronger influence of bases flanking much more mobile interface partners than was found earlier for regular uninterrupted duplexes by applying NN1 and NN2 models (41). These models were designed on the basis of melting data and were intended to predict duplex stability, taking into account the energy impact of hydrogen bonds, as well as stacking to immediate neighbors (NN1) or even long distance interactions with other neighbors (NN2). Another consideration is reordering of stacking in duplexes upon melting, when one of the interface bases becomes the last in remaining duplex.

It has to be stressed that our approach enabled us to determine thermodynamic parameters of coaxial stacking directly from experiments, similar to the study of stacking of dangling ends described earlier (18). Other approaches to calculate stacking energy based on interpretation of duplex stability measurements, or theoretical analysis of the NN1 model, are not reliable enough for the assessment of internal stacking and may even be incorrect for coaxial stacking. Indeed, duplex formation depends not only on stacking between bases, but also on hydrogen bonds, which makes interpretation of data especially complicated. This explains why our data do not correlate with coefficients determined by using the NN1 model, even if one takes into account the estimates of hydrogen bond energies by subtracting them from NN1 coefficients (40).

Our data do not correlate with the data on RNA coaxial stacking published by Turner's group either (4–6). The reason for this discrepancy is most probably radically different geometry of the A-form of RNA and B-form of DNA.

An important goal of this work was a comprehensive assessment of mismatch discrimination of interface bases using CSH. The efficiency of this discrimination proved to be surprisingly high. The impact of stacking sometimes exceeded the effect of missing hydrogen bonds, especially with the mismatch located on the pentamer side of the interface. This high efficiency of mismatch discrimination by CSH has been used for mutation detection on microchips by another group (28).

Another important goal of this work was to improve the SBH approach (CSH-SBH), particularly its recent development using MALDI-TOF MS (27). As we demonstrated earlier, MALDI-TOF MS-based analysis of microchips is capable of simultaneously detecting thousands of different substances in each gel pad, extending the effective length of immobilized oligonucleotides by the length of stacked oligomers. The findings presented in this paper can improve mutation detection and proofreading using MAGIChips™ in combination with MALDI-TOF MS. First, since FITC, and probably TR, effectively suppress stacking, they can be used to block tandem CSH hybridization where it interferes with accurate sequence determination. Secondly, two different methods of AT/GC equalization presented here can be applied for MAGIChip™-based analysis. The use of chaotropic agents (31,39,42) is inexpensive and convenient, though it results in some loss of discrimination capability; introduction of modified bases (31) is more expensive, but has high equalizing potential without compromising discrimination.

A widely used universal base, 5-nitroindole, cannot be used at terminal positions as a stacking or stabilizing base because it suppresses the discrimination ability. For CSH applications, it should be utilized inside the duplex. Therefore, it would be interesting to study the stacking behavior of other universal bases, particularly recently described bases with increased stacking C3-methylisocarbostyril and C5-methylisocarbostyril described by Berger *et al.* (43).

Another important fact established in this study is that single base overlaps, which can occur in the tiling method (27), are not energetically favorable and can be easily discriminated (see Table 2). Indeed, our earlier study of oligonucleotides bound by CSH on microchips and analyzed by MALDI-TOF MS (27) identified no overlapping oligonucleotides in the mass spectrum.

ACKNOWLEDGEMENTS

We thank B.Chernov for synthesis of amidites and oligonucleotides, S.Surzhikov for synthesis of TR-labeled oligonucleotides containing a 3′-amino group, Dr I.Taran for synthesizing other oligonucleotides, V.Chupeeva, A.Gemmell and E.Kreindlin for microchip manufacture and Dr V.Barsky for the fluorescence microscope design. We are grateful to Drs A.S.Zasedatelev, M.A.Livshits and A.Kolchinsky for critical reading of this manuscript, and to E.Novikova for editorial assistance. Health Front Line, Ltd (Champaign, IL) assisted in the preparation of this manuscript. This work was supported by grant 5/01 from the Russian Human Genome Program.

REFERENCES

1. Saenger,W. (1984) *Principles of Nucleic Acid Structure*. Springer Advanced Texts in Chemistry, Springer-Verlag, NY.
2. Pieters,J.M., Mans,R.M., van den Elst,H., van der Marel,G.A., van Boom,J.H. and Altona,C. (1989) Conformational and thermodynamic consequences of the introduction of a nick in duplexed DNA fragments: an NMR study augmented by biochemical experiments. *Nucleic Acids Res.*, **17**, 4551–4565.
3. Snowden-Ifft,E.A. and Wemmer,D.E. (1990) Characterization of the structure and melting of DNAs containing backbone nicks and gaps. *Biochemistry*, **29**, 6017–6025.
4. Walter,A.E. and Turner,D.H. (1994) The stability and structure of tandem GA mismatches in RNA depend on closing base pairs. *Biochemistry*, **33**, 12715–12719.
5. Walter,A.E., Turner,D.H., Kim,J, Lyttle,M.H., Muller,P., Mathews,D.H. and Zuker,M. (1994) Coaxial stacking of helixes enhances binding of oligoribonucleotides and improves predictions of RNA folding. *Proc. Natl Acad. Sci. USA*, **91**, 9218–9222.
6. Kim,J., Walter,A.E. and Turner,D.H. (1996) Thermodynamics of coaxially stacked helixes with GA and CC mismatches. *Biochemistry*, **35**, 13753–13761.
7. Katahira,M., Saeki,J., Kanagava,M., Nagaoka,M. and Uesugi,S. (1995) Comparative CD and thermodynamic studies between sheared A:G and Watson–Crick A:U(T) base pairs in RNA and DNA. *Nucleic Acids Symp. Ser.*, **34**, 59–60.
8. Lane,M.J., Paner,T., Kashin,I., Faldasz,B.D., Li,B., Gallo,F.J. and Benight,A.S. (1997) The thermodynamic advantage of DNA oligonucleotide 'stacking hybridization' reactions: energetics of a DNA nick. *Nucleic Acids Res.*, **25**, 611–617.
9. Roll,C., Ketterle,C., Faibis,V., Fazakerley,G.V. and Boulard,Y. (1998) Conformations of nicked and gapped DNA structures by NMR and molecular dynamic simulations in water. *Biochemistry*, **37**, 4059–4070.
10. Gellman,S.H., Haque,T.S. and Newcomb,L.F. (1996) New evidence that the hydrophobic effect and dispersion are not major driving forces for nucleotide base stacking. *Biophys. J.*, **71**, 3523–3526.
11. Sponer,J., Gabb,H.A., Leszczynski,J. and Hobza,P. (1997) Base–base and deoxyribose–base stacking interactions in B-DNA and Z-DNA: a quantum-chemical study. *Biophys. J.*, **73**, 76–87.

12. Florian,J., Šponer,J. and Warshel,A. (1999) Thermodynamic parameters for stacking and hydrogen bonding of nucleic acid bases in aqueous solution. *J. Phys. Chem. B*, **103**, 884–892.
13. Newcomb,L.F. and Gellman,S.H. (1994) Aromatic stacking interactions in aqueous solution: evidence that neither classical hydrophobic effects nor dispersion force are important. *J. Am. Chem. Soc.*, **116**, 4993–4994.
14. Hobza,P., Šponer,J. and Polasek,M. (1995) H-bonded and stacked DNA base pairs: cytosine dimer. An *ab initio* second-order Moeller–Plesset study. *J. Am. Chem. Soc.*, **117**, 792–798.
15. Friedman,R.A. and Honig,B. (1995) A free energy analysis of nucleic acid base stacking in aqueous solution. *Biophys. J.*, **69**, 1528–1535.
16. Kankia,B.I. and Marky,L.A. (1999) DNA, RNA and DNA/RNA oligomer duplexes: a comparative study of their stability, heat, hydration and Mg^{2+} binding properties. *J. Phys. Chem. B*, **103**, 8759–8767.
17. Norberg,J. and Nilsson,L. (1996) Influence of adjacent bases on the stacking–unstacking process of single-stranded oligonucleotides. *Biopolymers*, **39**, 765–768.
18. Bommarito,S., Peyret,N. and SantaLucia,J.,Jr (2000) Thermodynamic parameters for DNA sequences with dangling ends. *Nucleic Acids Res.*, **28**, 1929–1934.
19. Lysov,Y.P., Florentiev,V.L, Khorlin,A., Khrapko,K., Shick,V. and Mirzabekov,A.D. (1988) A new method to determine the nucleotide sequence by hybridizing DNA with oligonucleotides. *Proc. Acad. Sci. USSR*, **303**, 1508–1511.
20. Khrapko,K., Lysov,Y.P., Khorlin,A., Shick,V., Florentiev,V.L. and Mirzabekov,A.D. (1989) An oligonucleotide hybridization approach to DNA sequencing. *FEBS Lett.*, **256**, 118–122.
21. Khrapko,K., Lysov,Y.P., Khorlin,A., Ivanov,I., Yershov,G., Vasilenko,S., Florentiev,V.L. and Mirzabekov,A.D. (1991) A method for DNA sequencing by hybridization with oligonucleotide matrix. *DNA Sequence*, **1**, 375–388.
22. Lysov,Y.P., Chernyi,A.A., Balaev,A.A., Beattie,K.L., Florentiev,V.L. and Mirzabekov,A.D. (1993) Reconstruction of a sequenced sequence using results of stacked hybridization with an oligonucleotide matrix. *Mol. Biol. (Mosk.)*, **27**, 1126–1138.
23. Lysov,Y.P., Chernyi,A.A., Balaev,A.A., Gnuchev,F.N., Beattie,K.L. and Mirzabekov,A.D. (1994) Effectiveness of sequencing using stacking hybridization on oligonucleotide matrices with varying length of immobilized oligonucleotides. *Mol. Biol. (Mosk.)*, **28**, 832–839.
24. Lysov,Y.P., Chernyi,A.A., Balaeff,A.A., Beattie,K.L. and Mirzabekov,A.D. (1994) DNA sequencing by hybridization to oligonucleotide matrix. Calculation of continuous stacking hybridization efficiency. *J. Biomol. Struct. Dyn.*, **11**, 797–812.
25. Lysov,Y.P., Chernyi,A.A., Balaev,A.A., Gnuchev,F.N., Beattie,K.L. and Mirzabekov,A.D. (1995) Use of continuous stacking hybridization in sequencing using modified oligonucleotide matrices. *Mol. Biol. (Mosk.)*, **29**, 104–113.
26. Parinov,S., Barsky,V., Yershov,G., Kirrillov,E., Timofeyev,E., Belgovsky,A. and Mirzabekov,A. (1996) DNA sequencing by hybridization to microchip octa- and decanucleotides extended by stacked pentanucleotides. *Nucleic Acids Res.*, **24**, 2998–3004.
27. Stomakhin,A., Vasiliskov,V., Timofeev,E., Schulga,D., Cotter,R. and Mirzabekov,A. (2000) DNA sequence analysis by hybridization with oligonucleotide microchips: MALDI mass spectrometry identification of 5mers contiguously stacked to microchip oligonucleotides. *Nucleic Acids Res.*, **28**, 1193–1198.
28. Madonaldo-Rodriguez,R., Espinoza-Lara,M., Loyola-Abitia,P., Beattie,W.G. and Beattie,K.L. (1999) Mutation detection by stacking hybridization on genosensor arrays. *Mol. Biotechnol,* **11**, 13–25.
29. Fotin,A., Drobyshev,A., Proudnikov,D., Perov,A. and Mirzabekov,A. (1998) Parallel thermodynamic analysis of duplexes on oligodeoxyribonucleotide microchips. *Nucleic Acids Res.*, **26**, 1515–1521.
30. Proudnikov,D., Timofeev,E. and Mirzabekov,A.D. (1998) Immobilization of DNA in polyacrylamide gel for the manufacture of DNA and DNA–oligonucleotide microchips. *Anal. Biochem.*, **259**, 34–41.
31. Nguyen,N.K., Fournier,O., Asseline,U., Dupret,D. and Thuong,N.T. (1999) Smoothing of the thermal stability of DNA duplexes by using modified nucleosides and chaotropic agents. *Nucleic Acids Res.*, **27**, 1492–1498.
32. Haugland,R.P. (1992) *Handbook of Fluorescent Probes and Research Chemicals*, 5th Edn. Molecular Probes, Inc., Leiden, The Netherlands.
33. Guy,A., Ahmad,S. and Teoule,R. (1990) Insertion of the fragile 2′-deoxyribosylurea residue into oligodeoxynucleotides. *Tetrahedron Lett.*, **31**, 5745–5748.
34. Guschin,D., Yershov,G., Zaslavsky,A., Gemmell,A., Shick,V., Proudnikov,D., Arenkov,P. and Mirzabekov,A. (1997) Manual manufacturing of oligonucleotide, DNA and protein microchips. *Anal. Biochem.*, **250**, 203–211.
35. Timofeev,E., Kochetkova,S., Mirzabekov,A. and Florentiev,V. (1996) Regioselective immobilization of short oligonucleotides to acrylic copolymer gels. *Nucleic Acids Res.*, **24**, 3142–3148.
36. Barsky,Y., Grammatin,A., Ivanov,A., Kreindlin,E., Kotova,E., Barskii,V. and Mirzabekov,A. (1998) Wide-field luminescence microscopes for analyzing biological microchips. *J. Opt. Technol.*, **65**, 938–941.
37. Denisov,A.Y., Pyshnyj,D.V. and Ivanova,E.M. (2000) The nature of stabilization of the tandem DNA duplex pTGGAGCTG (pCAGC + (Phn-NH-(CH2)3-NH)pTCCA) based on the UV-, CD- and two-dimensional NMR spectroscopy data. *Bioorg. Khim.*, **26**, 373–386.
38. Wu,P. and Sugimoto,N. (2000) Transition characteristics and thermodynamic analysis of DNA duplex formation: a quantitative consideration for the extent of duplex association. *Nucleic Acids Res.*, **2**, 4762–4768.
39. Rees,W.A., Yager,T.D., Korte,J. and von Hippel,P.H. (1993) Betaine can eliminate the base pair composition dependence of DNA melting. *Biochemistry*, **32**, 137–144.
40. SantaLucia,J.,Jr, Allawi,H.T. and Seneviratne,P.A. (1996) Improved nearest-neighbor parameters for predicting DNA duplex stability. *Biochemistry*, **35**, 3555–3562
41. Doktych,M.J., Morris,M.D., Dormandy,S.J., Beattie,K.L. and Jacobson,K.B. (1995) Optical melting of 128 octamer DNA duplexes. Effects of base pair location and nearest neighbors on thermal stability. *J. Biol. Chem.*, **270**, 8439–8445.
42. Jacobs,K.A., Rudersdorf,R., Neill,S.D., Dougherty,J.P., Brown,E.L. and Fritsch,E.F. (1988) The thermal stability of oligonucleotide duplexes is sequence independent in tetraalkylammonium salt solutions: application to identifying recombinant DNA clones. *Nucleic Acids Res.*, **16**, 4637–4650.
43. Berger,M., Wu,Y., Ogawa,A., McMinn,D., Schultz,P. and Romesberg,F. (2000) Universal bases for hybridization, replication and chain termination. *Nucleic Acids Res.*, **28**, 2911–2914.